RESEARCH ARTICLE | JANUARY 15 2019

Development of sub-nanometer resolution depth-resolved XAFS/XMCD in the soft x-ray region towards operando measurements FREE

Kenta Amemiya ✉; Masako Sakamaki

AIP Conf. Proc. 2054, 040001 (2019)
https://doi.org/10.1063/1.5084602

Development of Sub-nanometer Resolution Depth-Resolved XAFS/XMCD in the Soft X-ray Region towards Operando Measurements

Kenta Amemiya[1,2,a)] and Masako Sakamaki[1,2,b)]

[1]*Institute of Materials Structure Science, High Energy Accelerator Research Organization, Tsukuba, Ibaraki 305-0801, Japan*
[2]*Department of Materials Structure Science, SOKENDAI (The Graduate University for Advanced Studies), Tsukuba, Ibaraki 305-0801, Japan*

[a)]Corresponding author: kenta.amemiya@kek.jp
[b)]masako.sakamaki@kek.jp

Abstract. Recent development of the depth-resolved X-ray absorption fine structure (XAFS) and X-ray magnetic circular dichroism (XMCD) techniques in the soft X-ray region is presented. A sub-nanometer resolution in the XAFS/XMCD measurement is achieved by collecting the Auger electrons at different detection angles, which correspond to different probing depths, but it is impossible to apply this technique under magnetic and/or electric fields because the electron trajectory is affected by the external fields. By adopting the fluorescence-yield detection mode using a soft X-ray CCD camera, the depth-resolved XAFS/XMCD technique under the external fields is realized, which leads to the operando measurements for the chemical and magnetic states at the surface and interface. The depth-resolved XAFS/XMCD measurement for an FeCo film under the magnetic field is demonstrated for the first time, which suggests that the ~15 ML-thick surface region consists of ~60% oxides with little magnetization.

INTRODUCTION

The depth profile of the chemical and magnetic states in ultrathin films have attracted much interest because the surface and interface play essential roles in the property of the whole film. For instance, Fe films grown on a Cu(001) substrate have been extensively studied in order to clarify the spin density wave state, whose wave vector is perpendicular to the film plane [1, 2, 3, 4, 5, 6]. The X-ray absorption fine structure (XAFS) and X-ray magnetic circular dichroism (XMCD) are powerful techniques for the element-specific observation of the chemical and magnetic states of ultrathin films, but the conventional XAFS/XMCD measurement has no depth resolution. To obtain chemical and magnetic information at the surface and interface separately from that in the inner layers, a depth-resolved XAFS/XMCD technique has been developed, which has a sub-nanometer resolution, and has been applied mainly to magnetic ultrathin films [5, 6, 7, 8].

Figure 1 illustrates principle of the depth-resolved XAFS/XMCD technique. In the soft X-ray region, X-ray absorption spectra are usually recorded in the electron-yield mode, in which the Auger electrons and secondary electrons, whose number is proportional to the X-ray absorption coefficient, are collected. The generated electrons are attenuated in the film before coming out to the vacuum with a typical attenuation length of several nm. Since the length of the electron path to the surface depends on the emission angle, the effective escape depth for the electrons is determined by the detection angle, θ_d. Therefore, the depth-resolved XAFS/XMCD technique is realized by collecting the Auger electrons at different θ_d, which corresponds to the different probing depths [5, 6, 8]. Figure 2 shows an example for the depth-resolved XMCD result [7]. The surface and inner-layer components of the XMCD spectra for an oxygen-covered Ni ultrathin film were separately estimated, and it was suggested that the surface single layer has a NiO-like structure, while the underlying inner layers are metallic.

Although the depth-resolved XAFS/XMCD technique in the electron-yield mode has a sub-nanometer depth resolution as shown in Fig. 2, it is impossible to obtain the data under magnetic and/or electric fields, because the

Proceedings of the 13th International Conference on Synchrotron Radiation Instrumentation – SRI2018
AIP Conf. Proc. 2054, 040001-1–040001-6; https://doi.org/10.1063/1.5084602
Published by AIP Publishing. 978-0-7354-1782-3/$30.00

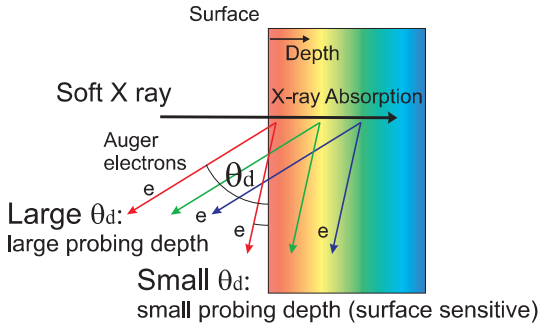

FIGURE 1. Principle for the depth-resolved XAFS/XMCD technique. The Auger electrons are collected at different detection angles, θ_d, which correspond to different probing depths for the XAFS/XMCD spectra.

electron trajectory is strongly affected by the fields. Therefore, only the remanent magnetic state had been investigated. Recently, to realize the depth-resolved measurement under the magnetic and/or electric fields, we have developed a fluorescence-yield depth-resolved XAFS/XMCD technique, in which the fluorescence X rays are detected at different θ_d, instead of the Auger electrons [9]. In the present contribution, the application of the fluorescence-yield depth-resolved XAFS/XMCD technique under a magnetic field is demonstrated. The surface and inner-layer components of the XAFS/XMCD spectra for an FeCo ultrathin film are separately estimated, and the depth-dependent chemical and magnetic states of the film are clarified.

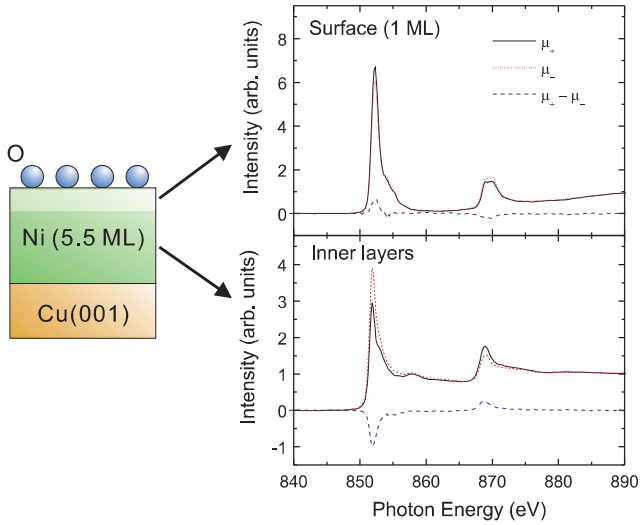

FIGURE 2. Surface and inner-layer components of Ni L-edge XMCD spectra for oxygen-covered Ni(5.5 ML)/Cu(001) estimated from a set of electron-yield XMCD spectra with different probing depths ranging from 0.6 to 1.0 nm [7]. It is assumed that the Ni film is divided into two regions, 1 ML-thick surface and underlying inner layers.

EXPERIMENTS

A FeCo film was prepared in a high vacuum chamber with a base pressure of 1×10^{-7} Pa. A Ag(001) single crystal was cleaned by repeated cycles of Ar^+ sputtering at 0.5 keV and subsequent annealing at ~450 K. A 30 ML (~4.3 nm)-thick FeCo film was grown at room temperature by a simultaneous deposition of Fe and Co by the electron bombardment

heating of Fe and Co rods. The film was then sputtered with 0.5 keV Ar^+, to reduce the oxidation of the film upon the exposure to the air [10]. The depth-resolved measurement was performed after the exposure of the film to the air for five years, which is long enough to stabilize the surface oxidation.

The depth-resolved XAFS/XMCD data were recorded at the soft X-ray beamline, BL-16A, of the Photon Factory, Institute of Materials Structure Science, High Energy Accelerator Research Organization, Japan [11]. Figure 3 illustrates the experimental setup for the depth-resolved XAFS/XMCD measurement. In the original setup, the Auger electrons were detected by an imaging-type electron detector, consisting of a microchannel plate, a phosphor screen, and a CCD camera for visible light, as shown in Fig. 3(a) [8]. On the other hand, in the present study, we adopted the fluorescence-yield mode, in which the fluorescence X rays emitted after the X-ray absorption were collected. The fluorescence X rays were detected at different θ_d by a soft X-ray CCD camera (Bitran BK-501X), whose detector elements were placed in vacuum, as shown in Fig. 3(b). The distance between the sample and the CCD camera was ~200 mm, and the detector size was 13×13 mm^2. Accordingly, the fluorescence X rays were simultaneously collected at $\theta_d = 0 - 2°$. Although the attenuation length for the fluorescence X rays is more than one order of magnitude larger than that for the Auger electrons, sub-nanometer probing depths were realized owing to the high spatial resolution of the CCD device, 13×13 μm^2 per pixel, as described below. A voltage of +1 kV was applied at the sample in order to prevent the Auger and secondary electrons from being detected by the CCD camera. The XMCD spectra were recorded at the normal-incidence configuration under a magnetic field of ~1000 Oe, which was generated by a pair of permanent magnets with 5 mm holes for X-ray beam, placed upstream and downstream of the sample. The direction of sample magnetization was fixed, and the polarization of the incident X rays was reversed to obtain the XMCD data.

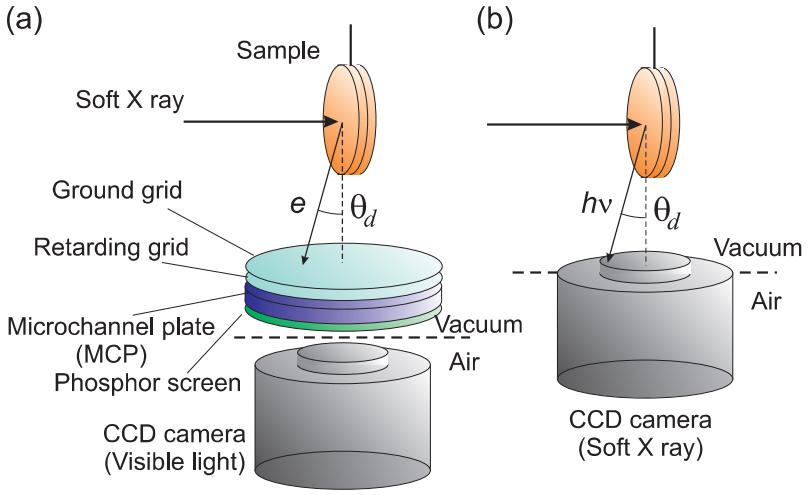

FIGURE 3. Experimental setup for the depth-resolved XAFS/XMCD technique in the (a) Auger-electron and (b) fluorescence-yield detection modes.

RESULTS AND DISCUSSION

Figure 4 shows probing depth dependence of the XAFS/XMCD spectra for the FeCo film taken in the fluorescence-yield mode. The probing depth, λ of each spectrum is determined as $\lambda = l\sin\theta_d$, where l denotes the attenuation length of the fluorescence X rays, which is ~300 nm [9]. One can recognize two peaks in the Fe L_3 region at ~707 and ~708 eV, as indicated by dashed lines, which are mainly attributed to Fe metal and oxides, respectively. Since the higher-energy component becomes more prominent at smaller probing depth, it is directly suggested that the surface of the film is oxidized. For the XMCD data, although the polarization dependence is rather small, it is suggested that magnetization of the film is reduced around the surface.

The obtained XAFS/XMCD spectra with different probing depths are then analyzed in order to estimate the surface and inner-layer components of the spectra. The energy, E, dependence of the number of the detected fluorescence

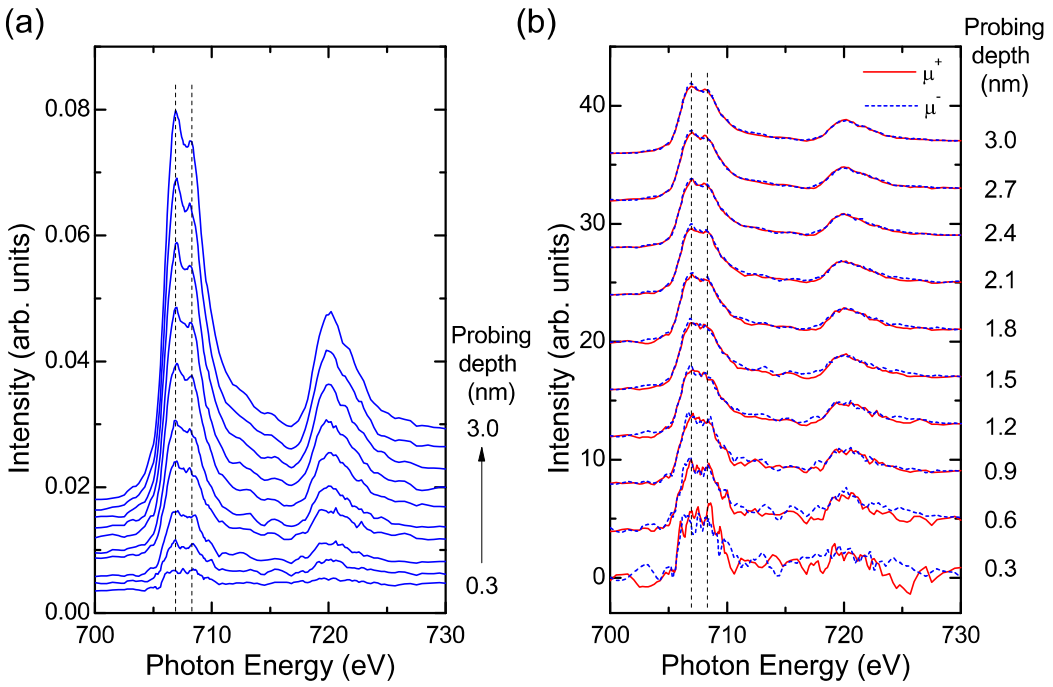

FIGURE 4. Fe L-edge (a) polarization-averaged and (b) XMCD spectra with different probing depths for FeCo film. The spectra shown in (b) are normalized to the edge-jump intensity.

X rays at λ, $Y(E,\lambda)$, is expressed by

$$Y(E,\lambda) = C\sum_{n=1}^{N}\mu_n(E)\exp\left(-\sum_{k=1}^{n-1}d_k\left(\frac{1}{\lambda}+\frac{1}{\cos\theta_{\text{in}}}\mu_k(E)\right)\right), \tag{1}$$

after the background subtraction, where C is the normalization factor, N is the film thickness in a ML unit, $\mu_n(E)$ is the X-ray absorption spectrum at the n th layer from the top, d_k is the layer spacing, and θ_{in} is the X-ray incidence angle from surface normal [9]. Here, the first and second terms in the exponential function correspond to the attenuations of the fluorescence and incidence X rays, respectively. In principle, the layer-resolved X-ray absorption spectra can be obtained by simultaneously optimizing all $\mu_n(E)$'s so as to reproduce the observed data set, $Y(E,\lambda)$'s, at all λ. For the XMCD spectra, $\mu_n(E)$ and $Y(E,\lambda)$ are substituted by $\mu_n^{\pm}(E)$ and $Y^{\pm}(E,\lambda)$, respectively, where $\pm$ represents the opposite circular polarizations.

However, the number of the fitting parameters is too large to be independently optimized, especially if the number of layers, n, is large. Therefore we assume that the FeCo film is divided into two regions, the surface and inner layers, and that the X-ray absorption spectrum within each region is identical;

$$\mu_n^{\pm}(E) = \begin{cases} \mu_{\text{surf}}^{\pm}(E) & (1 \le n \le t) \\ \mu_{\text{inner}}^{\pm}(E) & (t+1 \le n \le N) \end{cases}, \tag{2}$$

where t represents the thickness for the surface region, which is regarded as a fitting parameter. Moreover, we also assume that the polarization-averaged X-ray absorption spectrum for each layer is expressed by the linear combination of the standard spectra for Fe metal, Fe_3O_4, γ-Fe_2O_3, and α-Fe_2O_3 [12]. That is,

$$\frac{\mu_n^{+}(E)+\mu_n^{-}(E)}{2} = \sum_{m=1}^{M}c_{nm}\mu_m(E), \tag{3}$$

where $\mu_m(E)$'s are the standard spectra for Fe metal, Fe_3O_4, γ-Fe_2O_3, and α-Fe_2O_3, and the coefficients, c_{nm} and the XMCD difference spectra $\mu_n^+(E) - \mu_n^-(E)$ are simultaneously optimized.

Figure 5 shows surface and inner-layer components, $\mu_{surf}^{\pm}(E)$ and $\mu_{inner}^{\pm}(E)$, respectively, of the XMCD spectra estimated according to the above-described procedure. Here, we also assume that the inner layers consist of only the Fe metal component, and optimize the thickness of the surface region, t. On the other hand, the XMCD spectra, $\mu_n^+(E) - \mu_n^-(E)$, are optimized for both the surface and inner-layer regions. It is recognized that the surface region is dominated by oxides as indicated in Table 1. Moreover, the surface region shows little XMCD signal, while the inner layers show a significant XMCD. The optimized thickness of the surface region, t, is 15 ML, which is significantly smaller than that for the FeCo film without Ar^+ sputtering after the film deposition, which was reported to be 22 ML [9].

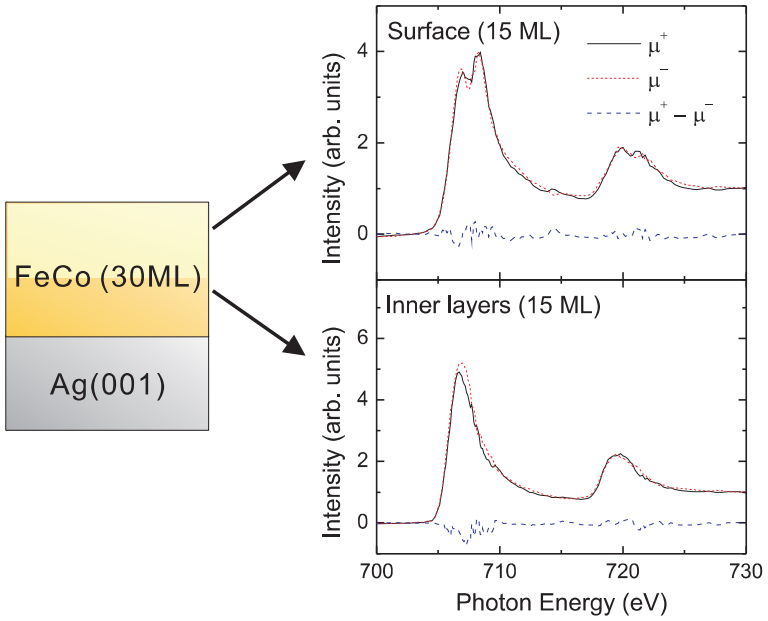

FIGURE 5. Surface and inner-layer components of Fe L-edge XMCD spectra for FeCo(30 ML)/Ag(001) estimated from a set of fluorescence-yield XMCD spectra with different probing depths. It is assumed that the inner layers consist of only the Fe metal component, and the thickness of the surface region, t, is optimized.

TABLE 1. Ratios of Fe metal, Fe_3O_4, γ-Fe_2O_3, and α-Fe_2O_3 components in the surface region.

Fe metal	**Fe_3O_4**	**γ-Fe_3O_4**	**α-Fe_2O_3**
0.42	0.0	0.38	0.20

CONCLUSION

Recent development of the depth-resolved XMCD technique in the soft X-ray region has been presented. The fluorescence-yield mode has been adopted, instead of the electron-yield mode, which enables us the depth-resolved analysis for the chemical and magnetic states under the magnetic and/or electric fields. Owing to the high spatial

resolution of the soft X-ray CCD camera for the detection of the fluorescence X rays, a sub-nanometer depth resolution was achieved. The technique was applied to the FeCo film, and its chemical and magnetic states around the surface were clarified from the depth-dependent XAFS and XMCD spectra. We have thus succeeded in the soft X-ray depth-resolved XMCD measurement under the magnetic field for the first time.

ACKNOWLEDGMENTS

The present work has been performed under the approval of the Photon Factory Program Advisory Committee (Nos. 2010S2-001, 2013S2-001, 2016S2-005, 2016G618, and 2016G628). The authors are grateful for the financial support of the Quantum Beam Technology Program, 2008–2012, and Grant-in-Aid for Scientific Research (Nos. 25287078, 15H02109, and 15K17684) from the Ministry of Education, Culture, Sports, Science and Technology, Japan (MEXT).

REFERENCES

[1] J. Thomassen, F. May, B. Feldmann, M. Wuttig and H. Ibach, Phys. Rev. Lett. **69**, 3831 (1992).
[2] D. Li, M. Freitag, J. Pearson, Z. Q. Qiu and S. D. Bader, Phys. Rev. Lett. **72**, 3112 (1994).
[3] D. Schmitz, C. Charton, A. Scholl, C. Carbone and W. Eberhardt, Phys. Rev. B: Condens. Matter **59**, 4327 (1999).
[4] D. Qian, X. F. Jin, J. Barthel, M. Klaua and J. Kirschner, Phys. Rev. Lett. **87**, 227204 (2001).
[5] K. Amemiya, S. Kitagawa, D. Matsumura, T. Yokoyama, and T. Ohta, J. Phys.: Condens. Matter **15**, S561 (2003).
[6] K. Amemiya, S. Kitagawa, D. Matsumura, H. Abe, T. Ohta, and T. Yokoyama, Appl. Phys. Lett. **84**, 936 (2004).
[7] K. Amemiya and M. Sakamaki, Appl. Phys. Lett. **98**, 012501 (2011).
[8] K. Amemiya, Phys. Chem. Chem. Phys. **14**, 10477 (2012).
[9] M. Sakamaki and K. Amemiya, Rev. Sci. Instrum. **88**, 083901 (2017).
[10] M. Sakamaki, K. Amemiya, A. Nambu, K. Ueda, J. Shimizu, and K.Watanabe, Mater. Chem. Phys. **143**, 281 (2013)
[11] K. Amemiya, A. Toyoshima, T. Kikuchi, T. Kosuge, K. Nigorikawa, R. Sumii, and K. Ito, AIP Conf. Proc. **1234**, 295 (2010).
[12] D. H. Kim, H. J. Lee, G. Kim, Y. S. Koo, J. H. Jung, H. J. Shin, J.-Y. Kim, and J.-S. Kang, Phys. Rev. B 79, 033402 (2009).